Journal of Advanced Research 44 (2023) 23–37

Contents lists available at ScienceDirect

Journal of Advanced Research

journal homepage: www.elsevier.com/locate/jare

Original Article

An miR156-regulated nucleobase-ascorbate transporter 2 confers cadmium tolerance via enhanced anti-oxidative capacity in barley

Nian-Hong Wang [a,1], Xue-Yi Zhou [a,1], Shou-Heng Shi [a], Shuo Zhang [a,b], Zhong-Hua Chen [c,d], Mohamed Abdelalim Ali [e], Imrul Mosaddek Ahmed [f], Yizhou Wang [a], Feibo Wu [a,b,*]

[a] Department of Agronomy, College of Agriculture and Biotechnology, Zijingang Campus, Zhejiang University, Hangzhou, 310058, PR China
[b] Jiangsu Co-Innovation Center for Modern Production Technology of Grain Crops, Yangzhou University, Yangzhou, 225009, PR China
[c] School of Science, Western Sydney University, Penrith, NSW, Australia
[d] Hawkesbury Institute for the Environment, Western Sydney University, Penrith, NSW, Australia
[e] Faculty of Agriculture, Microbiology Department, Cairo University, Giza, 2613, Egypt
[f] Plant Physiology Division, Bangladesh Agricultural Research Institute, Gazipur-1701, Bangladesh

HIGHLIGHTS

- microRNA expression compared in Cd-tolerant/sensitive barley Zhenong8 *vs* W6nk2.
- First report a novel gene *HvNAT2* targeted by miR156g-3p_3 vital in barley Cd tolerance.
- HvNAT2 evolved from the *Zygnematales* in *Streptophyte algae* and positively regulates Cd tolerance.
- Overexpression of *HvNAT2* enhances the expression of genes for ROS scavenging and antoxidative enzyme activity.

GRAPHICAL ABSTRACT

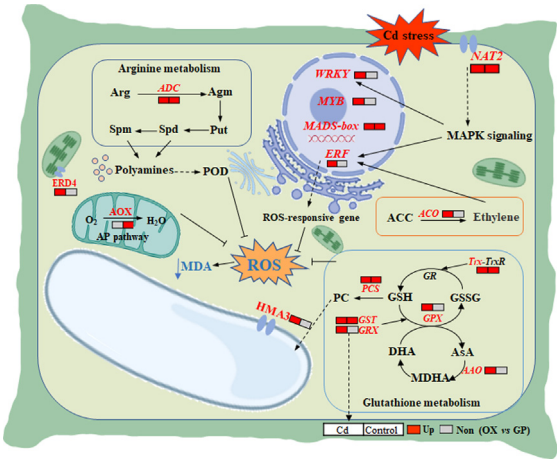

ARTICLE INFO

Article history:
Received 18 January 2022
Revised 29 March 2022
Accepted 5 April 2022
Available online 9 April 2022

Keywords:
miRNA
Cadmium toxicity
RNA sequencing
Oxidative signaling
Hordeum vulgare L

ABSTRACT

Introduction: Cadmium (Cd) is one of the most detrimental heavy metal pollutants, seriously affecting crop production and human health. Nucleobase-ascorbic acid transporters (NAT) are widely present in many living organisms including plants, animals and microbes; however, the role of NAT in plant Cd tolerance remains unknown.
Objectives: To identify Cd-induced miRNAs that target *HvNAT2* and to determine the role of this gene and its product in Cd tolerance.
Methods: High-throughput-sequencing was used to identify the miRNA expression profile of barley roots in response to Cd stress. Overexpression (OX) and RNAi lines were then constructed for *HvNAT2* and comparative transcriptomic analysis was performed to determine the function of this transporter examining its effects on traits such as Cd uptake/flux and translocation, morphology and antioxidant capacity in relation to Cd tolerance. In addition, phylogenetic analysis was performed to obtain insights into the

Peer review under responsibility of Cairo University.
* Corresponding author.
E-mail address: wufeibo@zju.edu.cn (F. Wu).
[1] These authors contributed equally to this article.

https://doi.org/10.1016/j.jare.2022.04.001

evolution of *HvNAT2*.
Results: Cd stress-induced genome-wide expression profiles of miRNAs identified a Cd-induced miRNA, miR156g-3p_3, that had *HvNAT2* as its target. *HvNAT2* was negatively regulated in the high-Cd-accumulating and Cd-tolerant genotype Zhenong8. Evolutionary analysis indicated that orthologues of the plasma membrane localized, *HvNAT2*, can be traced back to the sister group of land plants, the streptophyte algae. Overexpression of *HvNAT2* increases Cd tolerance with higher tissue Cd accumulation but less oxidative damage in transgenic barley plants. RNAi of *HvNAT2* leads to a significant reduction of Cd tolerance. The higher Cd accumulation in roots of the OX3 line was also demonstrated by confocal microscopy and electrophysiology. Transcriptome analysis showed that the enhancement of antioxidant capacity by *HvNAT2* was related to stress signaling pathways. Furthermore, oxidative stress tolerance in *HvNAT2*-OX plants was regulated by the synthesis of phytochelatins and the glutathione metabolism cycle.
Conclusion: Our study reveals a key molecular mechanism of NAT in Cd tolerance in plants that is useful for sustainable agricultural production and management of hazardous this heavy metal for better environment management and ecosystem function.

Introduction

Cadmium (Cd) is one of the most detrimental heavy metals. It has high soil to plant mobility, is readily absorbed by plants, and its accumulation in vegetative and reproductive organs is harmful to plant growth and development. When accumulated in the human body through the food chain, Cd can have devastating effects on human bones and kidney function and can even cause cancers [1]. Pollution of soil with Cd has become a serious global environmental issue, because it has been widely released into agricultural soils mainly due to the overuse of phosphate fertilizers and the application of sewage and other municipal wastes [2]. Large areas of arable land in countries such as China, Japan, Germany, the UK, and the USA, have been contaminated with different degrees of Cd pollution [3], causing concern in many industrialized and developing countries [4–6].

To cope with Cd toxicity, plants have evolved a series of adaptive strategies, including Cd exclusion, chelation by specific ligands, compartmentalization in vacuoles and, most importantly, activation of anti-oxidative defense and detoxification systems [7,8]. For instance, it was found that overexpression of *metallothionein 1e* (*OsMT1e*) enhances rice growth under Cd stress [9]. The roles of reactive oxygen species (ROS) scavenging systems in stress resistance have been studied in a number of systems. In rice, *glutathione S-transferase* (*OsGSTL2*) was found to enhance tolerance to heavy metals [10]. Using tobacco, Le Martret et al. [11] have shown that homoplasmic chloroplast transformants including those associated with dehydroascorbate reductase (DHAR), glutathione-S-transferase (GST) and glutathione reductase (GR) had alterations in ascorbate and glutathione levels leading to increased tolerance to abiotic stresses including Cd. However, a link between membrane transporters and oxidative stress genes has not been assessed in relation to Cd tolerance in crops such as barley.

Many studies have been designed to determine the relationship between transporter genes and Cd tolerance in plants. For example, P_{1B}-type heavy metal ATPases (HMA) are important for Cd transport in plant cells [12]. In *Arabidopsis thaliana* (L.) Heynh., AtHMA4 promotes root-to-shoot translocation of Cd, increasing Cd tolerance [13,14], and AtHMA3 is responsible for detoxifying Cd *via* vacuolar sequestration [15]. Natural variation in *ZmHMA3* results in differences in Cd accumulation in the grains of maize (*Zea mays* L.) [3], and a loss of function of a Ca^{2+}/H^{+} transporter (*CAX1*) in *Arabidopsis* leads to higher Cd sensitivity [16]. In barley (*Hordeum vulgare* L.), two zinc transporters (HvZIP3 and HvZIP8) are associated with low grain Cd accumulation [17], and a P-type ATPase (HvPAA1) mediates Cd tolerance [6]. However, the molecular mechanisms causing Cd tolerance and accumulation need further study. A better understanding of the relationship between gene function and tolerance to Cd will facilitate the development of green, healthy and sustainable development in agriculture as well as systems for phytoremediation.

Members of the nucleobase-ascorbic acid transporter (NAT) family have been found in various species. Maize leaf permease1 (ZmLPE1) was the first plant NAT transporter found to be related to chloroplast function [18,19] and has since been found in plants such as *Arabidopsis* [20], tomato (*Solanum lycopersicum* L.) [21] and apple (*Malus domestica* Borkh.) [22]. In *Arabidopsis*, there is high functional redundancy of NAT proteins, compared with the wild-type (WT), single, double and triple mutants have no obvious phenotypic differences in conditions such as strong light, ultraviolet light, and abiotic stress [20]. However, it was found that expression of apple *MdNAT2*, *MdNAT4* and *MdNAT6-11* changes during drought stress, and expression of *MdNAT1*, *MdNAT3-7*, *MdNAT9* and *MdNAT14* is inducible by salt stress [22]. Overexpression of *MdNAT7* was found to increase tolerance to drought and salt stress due to enhanced ROS scavenging and ion homeostasis [23,24].

Barley is a major cereal crop as feed or food, and is one of the main sources of direct or indirect human ingestion of Cd [25,26]. Previously, we identified two contrasting genotypes in Cd tolerance and accumulation, Zhenong8 (ZN8; a high-Cd-accumulating and Cd-tolerant genotype) and W6nk2 (a low-Cd-accumulating and Cd-sensitive genotype) [27]. Many genes have been reported to confer tolerance to Cd stress in barley [6,17,26], but it remains to be determined if NAT have a role in Cd tolerance in plants.

For this study, we hypothesized that HvNAT2 is regulated by a Cd-induced miRNA and improves Cd tolerance in barley *via* the regulation of oxidative stress. To determine if this is the case, high-throughput-sequencing was used to identify the miRNA expression profile of barley roots in response to Cd stress. miRNAs that target *HvNAT2* were then sought. Overexpression and RNAi lines were constructed for *HvNAT2* and comparative transcriptomic analysis was performed to determine the function of this transporter examining its effects on traits such as Cd uptake/flux and translocation, morphology and antioxidant capacity in relation to Cd tolerance. In addition, phylogenetic analysis was performed to obtain insights into the evolution of *HvNAT2*. Our results reveals that *HvNAT2* regulates Cd tolerance in barley *via* activation of anti-oxidative defense for tissue Cd tolerance; and provide a candidate gene being potential useful in genetic engineering of NAT in plants to develop Cd-hyperaccumulators for efficient phytoremediation on a large scale in badly contaminated sites to provide safer and cleaner soil for food production.

Materials and methods

Plant materials and experimental design

A hydroponic experiment was carried out in a greenhouse at Zhejiang University, Hangzhou, China. The barley genotypes used were Zhenong8 (ZN8) (a high-Cd-accumulating and Cd-tolerant genotype) and W6nk2 (a low-Cd-accumulating and Cd-sensitive genotype); the *cv*. Golden Promise (GP) was used for the construction of overexpression (OX) lines and RNA interference (RNAi) lines. Uniform barley grains were disinfected with 2% H_2O_2 for 20 min, washed 7 times with deionized water, then germinated in the dark on pierced lids of 5 L plastic drums full of deionized water at 20/18 °C (day/night). After 5 days, the water was replaced with 4.8 L basic nutrient solution (BNS), and only vigorously growing and uniform seedlings were preserved [28]. The solution's pH was adjusted to 5.8 ± 0.1 with HCl or NaOH as required and was constantly aerated with pumps. On the 3rd day after cultivation, the seedlings were treated with BNS + $CdCl_2$ (Cd) and treatment with BNS was used as a control for both genotypes. A split-plot design was used with treatment as the main plot and genotype as the sub-plot with four replicates for each treatment. After 24 h of treatment, the roots from each replicate were sampled, immediately put into liquid nitrogen and stored at −80 °C for RNA extraction.

RNA and miRNA sequencing and data analysis

RNA sequencing and data analysis in barley were implemented as described in Qiu et al. [29]. Total RNA was extracted using TRIzol Reagent (Invitrogen, USA). PolyA tail mRNA was enriched by magnetic beads containing OligodT sequences. The RNA obtained was then broken into fragments using interrupt buffer. Finally, a single-stranded circular DNA library was obtained using random primers and adapters and sequenced by DNBSEQ. After cleaning the adaptor contaminants, low quality reads and reads with N ratio greater than 5%, Bowtie2 were used to align clean reads to the genome sequence and RSEM was used to calculate the gene expression level of each sample. DEseq2 was employed to determine differences between groups, sequences with a |fold change| $\geq$1 and Q < 0.0001 were considered to be differentially expressed.

Construction of microRNA (miRNA) libraries and Illumina sequencing were also implemented according to Qiu et al. [29]. After elimination of adapter sequences and low quality sequences, clean reads were compared to the barley reference genomes and other miRNA databases. Novel miRNAs were predicted using RIPmiR, and DEGseq was used to analyze the differential expression. The miRNAs were determined to be up-regulated if they had a $\log_2N \geq 1$, down-regulated if $\log_2N \leq -1$; those with $0 < |\log_2N| < 1$ were determined to be unchanged, $Q \leq 0.001$. Target genes of miRNAs were predicted by psRobot (http://omicslab.genetics.ac.cn/psRobot/) and TargetFinder, using default parameters.

For miRNAs, RNA samples were reverse-transcribed using a miRNA 1st Strand cDNA Synthesis Kit (by stem-loop) (Vazyme) and followed by qRT–PCR using miRNA Universal SYBR qPCR Master Mix (Vazyme) with 18S rRNA as the internal control. For gene expression, a PrimeScript™ II 1st strand cDNA synthesis kit (Takara) was used for reverse transcription of RNA samples, followed by SYBR Premix Ex Taq Kit (Takara) with *HvGAPDH* as the internal control. qRT–PCR reaction was performed on LightCycler 480 System (Roche, Germany). All primers used are listed in Tables S1-S2.

Evolutionary and phylogenetic analysis

Evolutionary bioinformatics were implemented as described by Feng et al. [30]. Candidate protein sequences of NAT2 were identified in the 1000 Plant Transcriptome (1KP; https://www.onekp.com) database [31]. A phylogenetic tree was structured with Fast Tree and annotated by Interactive Tree of Life resource (https://itol.embl.de/). Protein sequences were aligned by Jalview. Functional domains and three-dimensional structures were predicted with SMART (https://smart.embl-heidelberg.de/), Protter (https://wlab.ethz.ch/protter/start/) and SWISS-MODEL (https://swissmodel.expasy.org/).

Molecular biology

The DNA sequence of *HvNAT2* was acquired from Ensembl (http://plants.ensembl.org/Hordeum_vulgare/Info/Index), and primers were subsequently designed to amplify the coding sequence in ZN8 and W6nk2, and the resulting amplicons were ligated into pMD18-T vector (Takara, Japan) and sequenced.

The subcellular location of *HvNAT2* was determined according to Wang et al. [6]. The coding region of *HvNAT2* (without termination codon) was amplified using the cDNA of ZN8 as the template and ligated to the CAMBIA1300-35S-sGFP vector containing the green fluorescent protein (GFP) tag. *In situ* PCR analysis was implemented as described by Feng et al. [30], using alkaline phosphatase-conjugated anti-digoxin Fab fragment and BM Purple AP substrate (Roche, Penzberg, Germany) for color rendering. *HvActin* was used as the positive control.

Roots, stems, first and third leaves of 20-days-old seedlings were sampled for analysis of the tissue expression of *HvNAT2* in ZN8 without Cd. In a time-dependent *HvNAT2* expression experiment, two-leaf stage seedlings of ZN8 were treated with 0 or 10 μM Cd, then the leaves were sampled 0, 1, 3, 6, 12, 24, 48 and 72 h after Cd treatment. For the assessment of *HvNAT2* overexpression and RNAi transgenic lines, leaves were sampled 30 and 15 d after the 0 or 10 μM Cd treatments. The expression of *HvNAT2* was quantified by qRT-PCR, using *HvGAPDH* as an internal control. All primers used are listed in Table S3.

Barley transformation was implemented as described by Shen et al. [32]. Using Gateway technology (Invitrogen, USA), full length CDS and 427 bp interference segment of *HvNAT2* were amplified by PCR and cloned into pDONR-Zeo (Invitrogen) and mobilized into the vectors pBract214 and pANDA that contain a ubiquitin promoter. Afterwards, the two vectors were transformed into the *Agrobacterium* strain AGL1 (pSounp). Immature embryos of GP were separated 2–3 weeks after flowering and placed on CI medium for 3–4 days. Then the embryos were soaked with *Agrobacterium* and co-cultured for 2–3 days before being placed on a selective culture medium containing hygromycin and termin to select for transgenic seedlings. DNA of all transgenic barley lines was extracted for verification of transgenicity by PCR. Three positive overexpression lines, two silencing lines, and transformation-free GP were used for further experiments. The expression levels of *HvNAT2* were also determined by qRT-PCR.

Physiological measurements

The overexpression and RNAi lines were sampled and measured 30 d and 15 d after 10 μM Cd treatments. A chlorophyll meter (Minolta SPAD-502 developed by the Soil–Plant Analyses Development (SPAD) Section of Minolta Camera Co., Ltd., Osaka, Japan) was used to determine relative chlorophyll contents of the 4th fully expanded functional leaves from the apex. The roots were immersed in 15 mM disodium ethylenediamine tetra-acetic acid (Na_2-EDTA) solution for 60 min to remove the surface ions, and washed with deionized water before determination of the root length [6]; shoot height was also determined at this time. Roots were assessed with a root scanner to determine total root length,

total volume, total surface area and average diameter. The shoots and roots were dried at 110°C for 1 h then at 70 °C for 5 d to measure dry weight [6]. Cd, Fe, Mn, Cu and Zn content in roots and shoots was measured using inductively coupled plasma optical emission spectroscopy (ICP-OES) (Optima8000DV, PerkinElmer, USA). Using methods by Wu et al. [28] and Chen et al. [33,34], fresh leaves and roots were used to measure superoxide dismutase (SOD), glutathione peroxidase (GPX), ascorbate peroxidase (APX), glutathione-S-transferase (GST) and peroxidase (POD) activities and malondialdehyde (MDA). Glutathione (GSH) contents was assayed colorimetrically using a Reduced Glutathione Content Assay Kit (Sangon Biotech), and nitric oxide (NO) content was measured by the nitrate reductase method using a NO assay kit (Nanjing Jiancheng Bioengineering Institute).

Fluorescence imaging

Fluorescence imaging was performed according to Cao et al. [4]. Root tips taken 15 d after 0 or 10 μM Cd treatments were immersed in Na_2-EDTA for 20 min and washed five times with deionized water. Then roots were soaked in the Cd probe Leadmium Green AM solution (Molecular Probes, Life Technologies, California, USA) for 90 min in the dark. Sections were observed by laser confocal scanning microscope (Leica TCS SP5; Germany) using 488 nm excitation wavelengths and 515 nm emission wavelengths. The images were analyzed by Image J.

Net ion flux measurements

Net Cd^{2+} fluxes were determined by noninvasive ion-selective microelectrode ion flux estimation (MIFE) (University of Tasmania, Hobart, Australia) according to Mak et al. [35]. Roots of intact barley seedlings were stabilized in a horizontal chamber with testing solution (0.5 mM KCl + 0.1 mM $CaCl_2$) for 1 h before Cd^{2+} flux measurements. Microelectrodes were top-excised to 2 to 3 μm in diameter, then back-filled with 1 M KCl and 10 mM $CdCl_2$ and front-filled with an ion-selective Cd^{2+} cocktail. The cocktail was freshly prepared with Cd^{2+} ionophore I, potassium tetrakis, and 2-nitrophenyl octyl ether (Cat. Nos 20909, 60588, and 73732; Sigma-Aldrich) according to Piñeros et al. [36]. Net Cd^{2+} fluxes were gauged from root mature zone for 5 min to acquire the constant initial flux value. Soon afterwards, the testing solution was replaced with the 10 μM $CdCl_2$, and transient ion flux measurements obtained for another 25 min. Net Cd^{2+} fluxes were then computed by cylindrical diffusion geometry using the MIFEFLUX program. Ten replications of each barley line were assayed.

Statistical analysis

Data were the averages of three to ten biological replicates, and were analyzed by ANOVA, followed by comparisons of means using Tukey's test. Statistical analyses were performed using SPSS Statistics.

Results

Identification of HvNAT2 as a target of Cd tolerance-related miRNAs in barley

We first conducted miRNA sequencing to identify miRNAs and their predicted target genes underlying Cd tolerance in ZN8 (Fig. 1; Figs S1-S2; Tables S4-S8). Among the 72 conserved miRNAs in both genotypes, 11 miRNAs were down-regulated in W6nk2 but not in ZN8, and 18 miRNAs were unchanged in W6nk2 but up-regulated in ZN8 (Fig. 1A; Table S6). In addition, 8 miRNAs were down-regulated in ZN8 but not in W6nk2, while 5 miRNAs were unchanged in ZN8 but up-regulated in W6nk2 (Fig. 1A; Table S7). Out of 31 novel miRNAs, 2 miRNAs were down-regulated in W6nk2 but unchanged in ZN8; 8 miRNAs were unchanged in W6nk2 but up- or down-regulated in ZN8 (Table S8). Some of the miRNAs appeared not to interact with any genes in our study, and combined with target prediction and their target genes changes, only 17 miRNAs-mRNA pairs were simultaneously interacted in both two genotypes in response to Cd stress. We considered these 17 miRNA-mRNA pairs to be related with Cd tolerance in ZN8 (Fig. 1B). To corroborate the high-throughput sequencing data, 6 miRNAs were stochastically chosen and their expression levels were confirmed by qRT–PCR (Fig. S3A-F).

Among the miRNAs associated with Cd treatment, miR156g-3p_3 was up-regulated by Cd treatment in ZN8, but unchanged in W6nk2 (Fig. 1B; Table S6), indicating its potential involvement in responses to Cd stress. One of the target genes of miR156g-3p_3 was determined to be *HvNAT2*, whose protein participates in redox reactions; therefore, *HvNAT2* was subjected to evolutionary and functional exploration. The miRNA was predicted to cleave the 5′ end of the product (Fig. 1C) Fig. S3. A time-course experiment using leaves showed that *HvNAT2* expression was quickly induced by Cd treatment, reaching it highest expression at 1 h after the imposition of Cd stress and then gradually decreased (Fig. 1D).

Plasma membrane NAT2 is a nucleobase-ascorbate transporter evolved from streptophyte algae

Bioinformatics and evolutionary tools were used to evaluate NAT2 and the NAT gene family of plant and algal species. The full-length genomic DNA of *HvNAT2* was 3,980 bp, with 14 exons and 13 introns (Fig. 1C). The full-length coding sequence of *HvNAT2* was 1,575 bp, encoding a protein containing 524 amino acids with a predicted molecular weight of 57.15 kDa and a theoretical pI 8.13. HvNAT2 was predicted to contain 11 transmembrane domains (TMD); this is consistent with 10–12 TMD in other members of the NAT family (Fig. 2A).

Using sequences in the OneKP plant transcriptome database, we showed that orthologues of HvNAT2 are found in major lineages of plants and algae and that HvNAT2 is closely related to TaNAT2 in wheat (*Triticum aestivum* L.) and AetNAT2 in *Aegilops tauschii* Coss. (Fig. 2B). HvNAT2 could be placed into Subfamily Ⅱ and was predicted to be a transporter with high affinity for oxidized purines, xanthine and uric acid but not ascorbic acid (Fig. 2C). The orthologues of HvNAT2 could be traced back to streptophyte algae such as *Zygnemopsis* sp. (*Zygnematales*), implying an evolutionary origin of NAT2 from this group, the sister clade to land plants. Logo analysis of the key domains NAT2 showed that they are highly conserved among the representative species of angiosperm, gymnosperm, fern, lycophyte, moss, liverwort and streptophyte algae (Fig. 2D-E) in the database. Most interestingly, the NAT signature domain, (Q/E/P)NXGXXXXT(R/K/G), was found in streptophyte algae but not in chlorophyte algae.

In addition, the expression level of *HvNAT2* in leaves was higher than in stems and roots (Fig. 3A). The subcellular localization analysis of HvNAT2 in tobacco leaf epidermis showed that it was localized in the plasma membrane (Fig. 3B). In situ PCR assays of barley tissues demonstrated that the DIG staining signals were recorded in almost all parts of root cells but a little bit more expressed in vascular bundles (Fig. 3C). In leaves, HvNAT2 was mainly expressed in vascular bundles particularly in phloem cells (Fig. 3D).

Overexpression of HvNAT2 enhanced Cd tolerance in barley

To confirm the function of *HvNAT2*, we generated three independent overexpression lines *HvNAT2*-OX1, *HvNAT2*-OX2 and

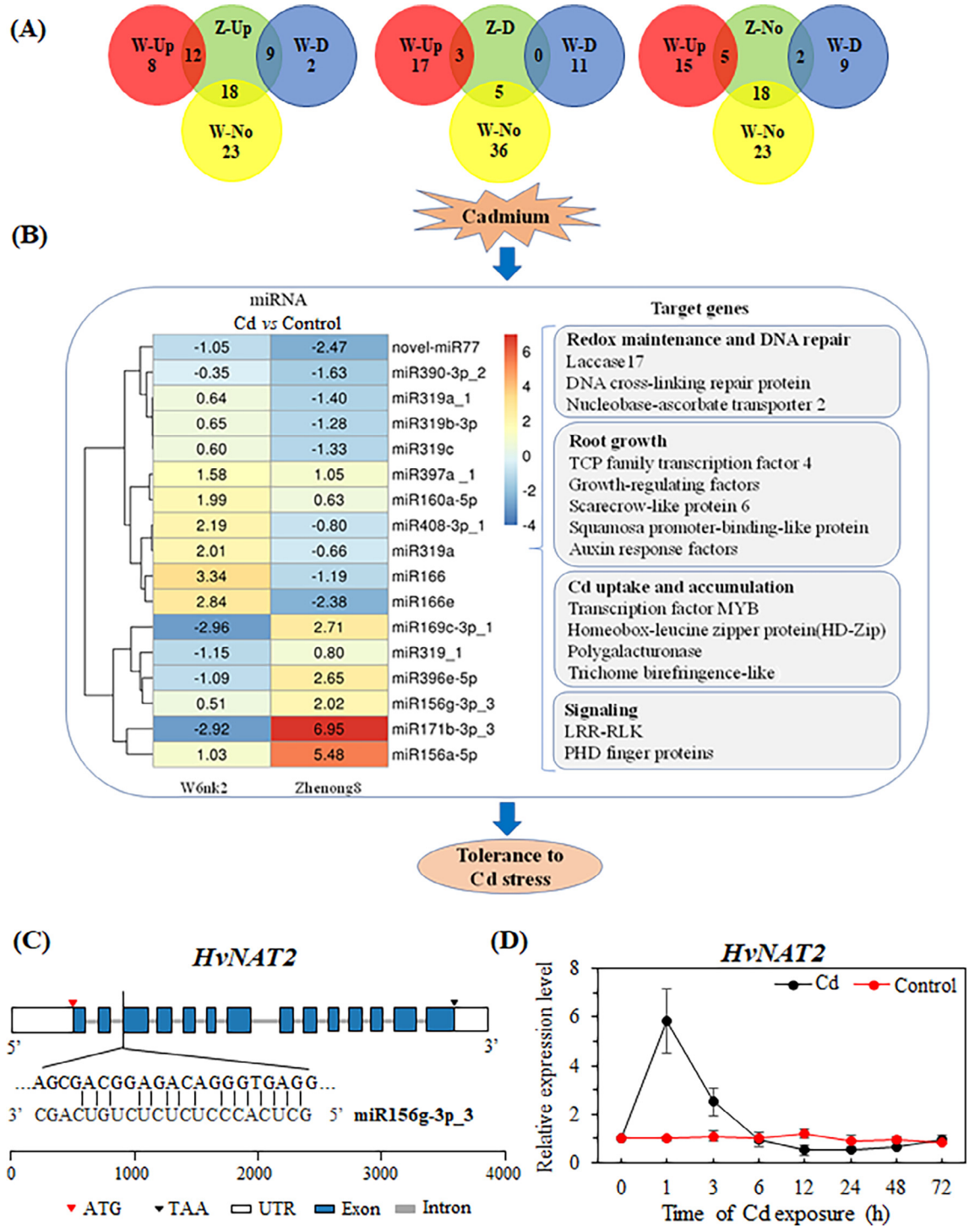

Fig. 1. Schematic diagram of Cd-induced miRNAs and target genes and target validation of miR156g-3p_3 in barley. (A) Venn diagrams show the number of miRNAs regulated by 5 μM Cd treatment and overlap between the W6nk2 (W) and Zhenong8 (Z). The overlaps represent the expression of miRNAs in W6nk2, which were up-regulated (Up), down-regulated (D) and unchanged (No) in Zhenong8. (B) Hypothetical schematic diagram of Cd tolerance mechanism in Zhenong8 regulated involving miRNA and their target genes. Fold change (Cd *vs* control) is $\log_2$N, $\log_2 N \geq 1$ are up-regulated, $0< |\log_2 N| < 1$ are unchanged and $\log_2 N \leq -1$ are down-regulated, $Q \leq 0.001$. (C) Gene structure of *HvNAT2* and location of mature sequence of miR156g-3p_3 targeting mRNA of *HvNAT2*. The white box means the untranslated region (UTR), blue box represents the exon and gray line represents intron. Arrowhead represents the translation start and stop sites. (D) Time dependent expression of *HvNAT2* in Zhenong8 in response to Cd treatment.

HvNAT2-OX3 (Fig. 4A). The transcript levels of *HvNAT2* in the OX lines were on average 37-fold and 34-fold higher than GP under control conditions and when subjected to Cd treatment, respectively (Fig. 4B). In contrast to the control, 30 d of Cd stress significantly caused a reduction in plant dry weight of 60.2% in GP compared to the control; the corresponding reduction was 43.5% in the OX lines (Fig. 4C). Chlorophyll contents (as determined by SPAD values), tiller numbers, total root lengths, root volumes and root tip numbers of the OX lines were significantly greater than those of GP under Cd stress (Fig. 4D-E; Fig. S4; Table S9). Strikingly,

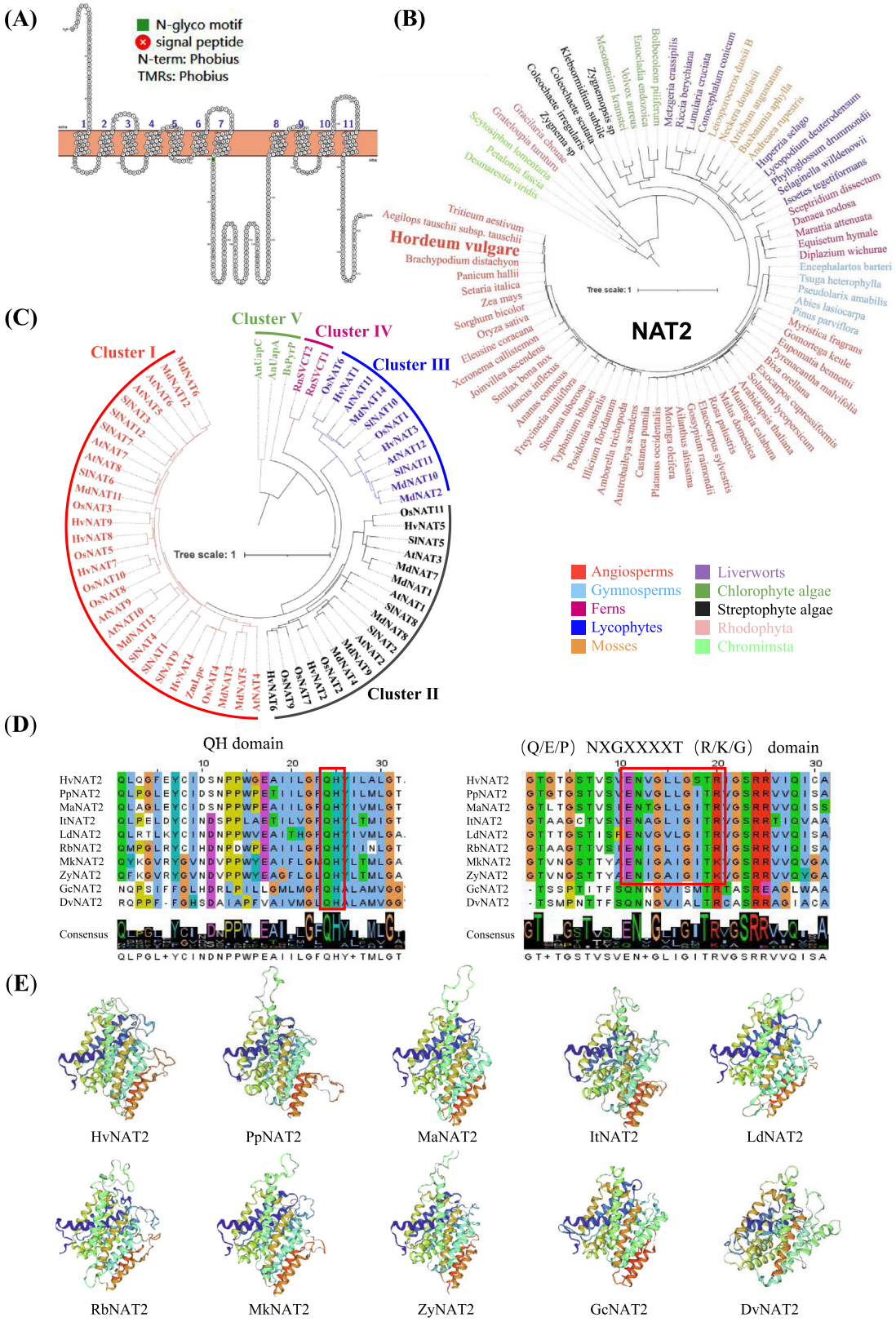

Fig. 2. Evolutionary and structural analysis of NAT2 in green plants. (A) Transmembrane domain prediction of HvNAT2 *via* Protter. (B) Phylogenetic tree of NAT2 proteins in plants and algae. The neighbor-joining (NJ) method was used to construct the tree. (C) Phylogenetic analyses of NAT family by NJ method. The tree includes NATs of *Hordeum vulgare* (Hv), *Arabidopsis thaliana* (At), *Oryza sativa* (Os), *Solanum lycopersicum* (Sl), *Malus domestica* (Md), *Zea mays* (Zm), *Mesembryanthemum crystallinum* (Mc), *Rattus norvegicus* (Rn), *Bacillus subtilis* (Bs) and *Aspergillus nidulans* (An). Clades are highlighted as I–V. (D) Alignment of the two conserved domains of NAT2 in ten typical plant and algal species. (E) Predicted three-dimensional structure of NAT2 in the ten typical plant and algal species. Hv, *Hordeum vulgare*; Pp, *Pinus parviflora*; Ma, *Marattia attenuata*; It, *Isoetes tegetiformans*; Ld, *Leiosporoceros dussii_B*; Rb, *Riccia berychiana*; Mk, *Mesotaenium kramstei*; Zy, *Zygnemopsis*; Gc, *Gracilaria chouae*; Dv, *Desmarestia viridis*.

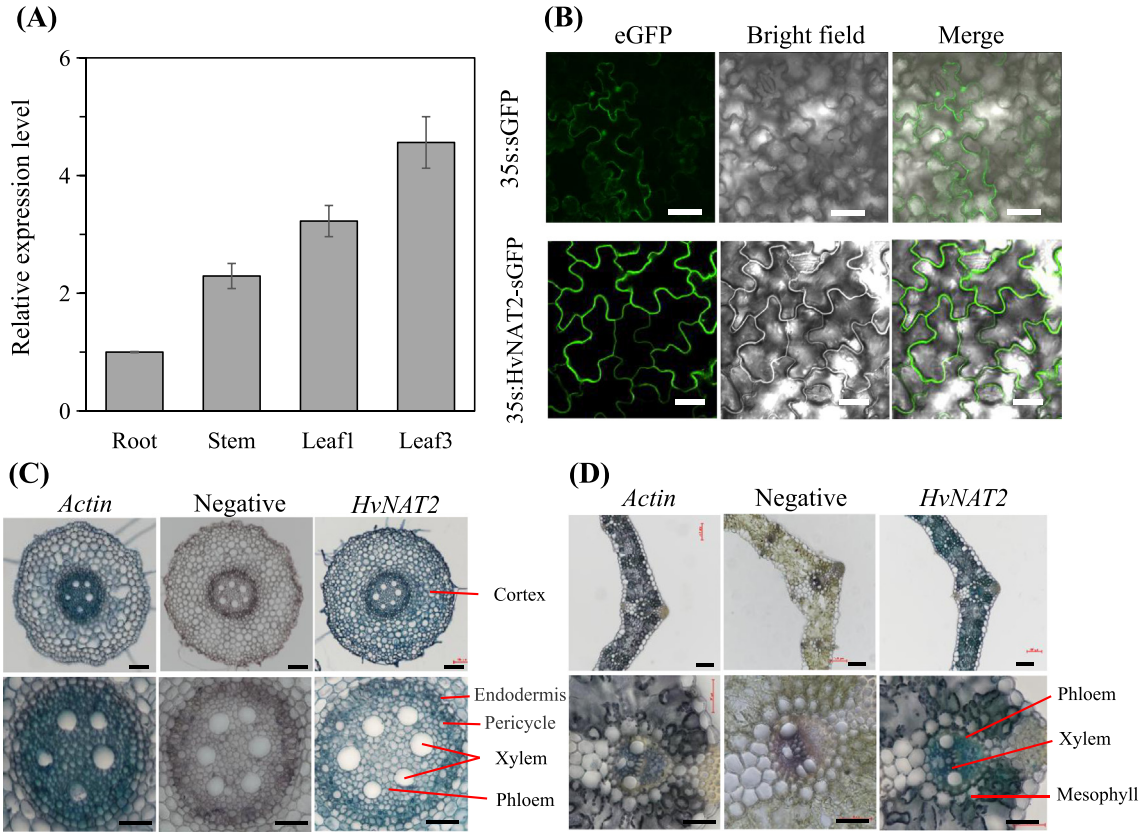

Fig. 3. Expression patterns and subcellular localization of *HvNAT2*. (A) qRT-PCR analysis of the relative transcript levels of *HvNAT2* in different tissues of Zhenong8. *HvGAPDH* was used as internal control. (B) Subcellular localization of *HvNAT2* by transient expression in tobacco leaves. The signals were examined using a fluorescence microscope. sGFP, green fluorescent protein. Cell images were also observed under bright field as a control. (C, D) Tissue localization of *HvNAT2* in roots (C) and leaves (D) of Zhenong8 by *in situ* PCR. All samples were stained with BM Purple. The blue color means the presence of digoxigenin (DIG)-labeled cDNA. *Actin* gene was used as a positive control. Typical images are shown out of five replicates. Bars = 50 μm.

under Cd stress, overexpression of *HvNAT2* result in significant increases of Cd concentration by 45.7% and 51.3% in shoots and roots, respectively (Fig. 4F) and greater Cd fluorescence signals in roots compared with GP (Fig. 5A-B).

Addition of 10 μM $CdCl_2$ resulted in a rapid Cd^{2+} influx with the highest transit flux recorded in *HvNAT2*-OX3 plants as compared to GP (Fig. 5C). Further analyses of Cd^{2+} influxes showed that *HvNAT2*-OX3 has significantly higher total and average fluxes (31% and 39%, respectively; $P \leq 0.05$) compared to GP (Fig. 5C). Moreover, overexpression of *HvNAT2* significantly reduced the contents of shoot Fe and Cu and root Mn, Fe, and Zn on a dry weight basis, but increased the overall accumulation of Mn, Cu and Zn per plant compared with GP under Cd stress. Interestingly, the root-to-shoot transport rates of Mn, Fe and Zn were significantly higher compared with GP under Cd stress (Fig. S5).

Suppression of HvNAT2 reduces Cd tolerance in barley

We subsequently examined the function of *HvNAT2* using two RNAi lines (*HvNAT2*-RNAi1 and *HvNAT2*-RNAi2) (Fig. 6A), which had on average 47% and 51% lower expression of *HvNAT2* compared with GP under the control and Cd treatment, respectively (Fig. 6B). Reduction of *HvNAT2* expression in *HvNAT2*-RNAi1 and *HvNAT2*-RNAi2 resulted in a Cd sensitive phenotype (Fig. 6C-D) compared to the control. On average, the two *HvNAT2*-RNAi lines shoot and root dry weights were reduced by 40.1% and 55.3% after 15 d Cd stress, but the corresponding reduction was 22.0% and 28.9% in GP (Fig. 6E-F). The *HvNAT2* RNAi lines showed significant decreases in root Cd concentrations and plant Cd accumulation, but significantly higher root-to-shoot Cd transport rates compared with GP (Fig. 6I-K). The significant decrease in Cd accumulation in roots of *HvNAT2*-RNAi1 was validated by Cd green fluorescence (Fig. 5A-B), and ion flux measurements showed that steady-state Cd^{2+} flux from roots of *HvNAT2*-RNAi1 was significantly decreased by 23% compared to that of GP (Fig. 5C). Moreover, suppression of *HvNAT2* significantly reduced the contents of shoot Fe and root Fe and Cu along with the overall accumulation of Mn, Cu and Zn per plant compare with GP under Cd stress. The root-to-shoot transport rates were variable, showing significantly higher Cu and lower Fe compared with GP under Cd stress (Fig. S6).

HvNAT2 regulates expression of redox-related genes to enhance Cd tolerance

To reveal potential Cd-tolerance mechanisms regulated by *HvNAT2*, we conducted RNA-sequencing experiments of GP and *HvNAT2*-OX lines under control and Cd stress through transcriptome analysis (Fig. 7A; Table S10). We identified 173 differentially expressed genes (DEGs) in GP and OX plants in response to Cd treatment (Fig. 7B; Table 1; Table S11). The RNA-seq results were validated by qRT-PCR analysis for 26 differentially expressed genes in OX lines and GP under control and Cd and 6 random selected barley genes (Tables 1, S2; Fig. S7). Gene Ontology (GO) analysis revealed that these DEGs mainly participate in cellular processes, metabolic processes, molecular function regulation, response to stimuli, signaling, and redox related in ROS regulation (Fig. 7C).

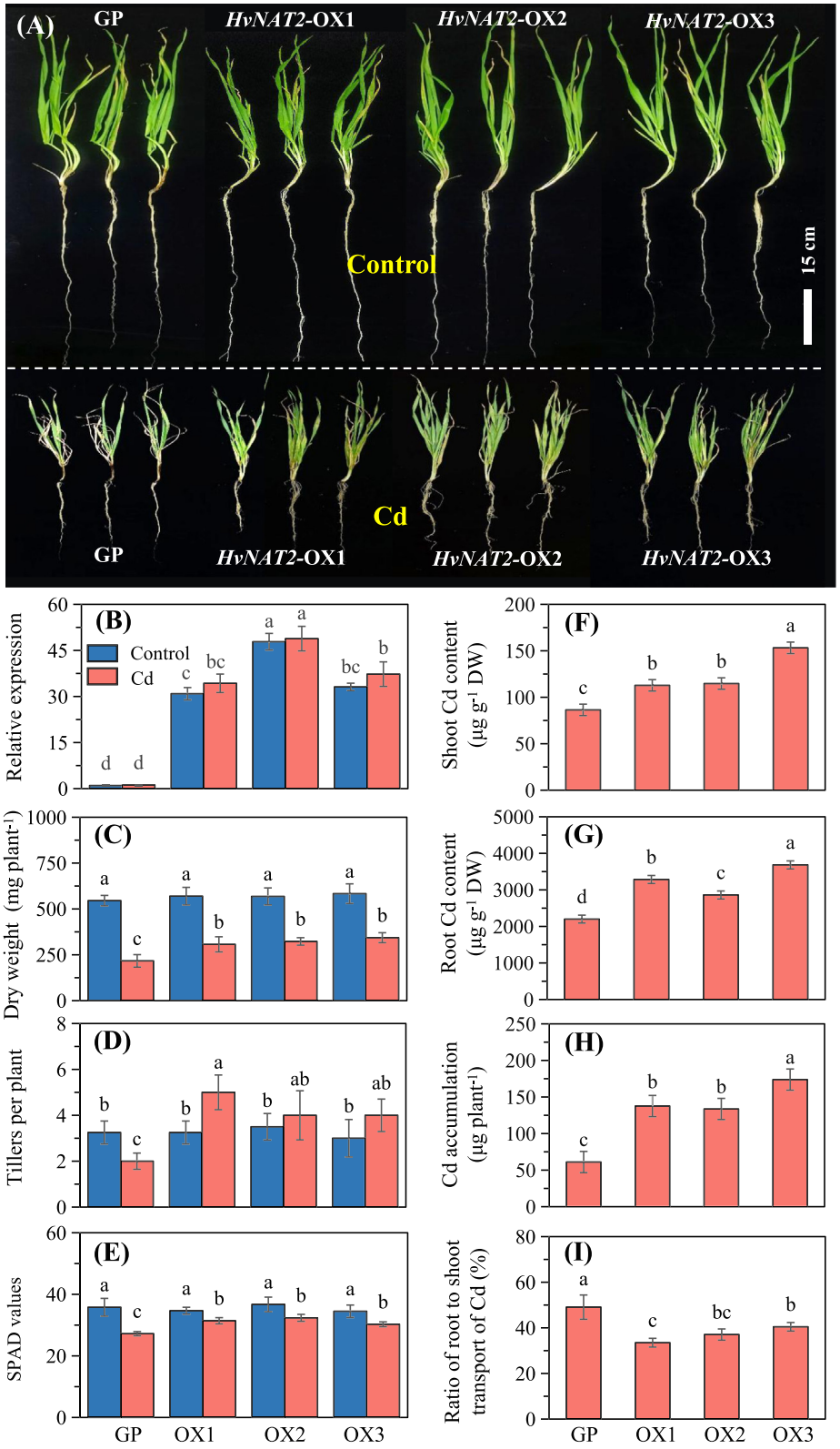

Fig. 4. Functional assessment of *HvNAT2 via* gene overexpression in barley. (A) Phenotype of Golden Promise (GP) and *HvNAT2*-OX lines (OX1, OX2, OX3) under control and Cd stress conditions. (B) Relative expression of *HvNAT2*. *HvGAPDH* was used as internal control which was described in Molecular Biology of materials and methods. (C-E) dry weight (C), tillers per plant (D), relative chlorophyll content (SPAD) (E) of GP and *HvNAT2*-OX lines. (F-I) Shoot Cd concentration (F), root Cd concentration (G), Cd accumulation (H) and ratio of root to shoot transport (I) of GP and *HvNAT2*-OX lines. Plants were exposed to 0 or 10 μM Cd for 30 days. Data are means ± SD of three biological replicates and different letters stand for significantly different at $p \leq 0.05$.

KEGG enrichment revealed that these genes are involved mainly in plant-pathogen interaction, mRNA surveillance pathway, mitogen-activated protein kinase (MAPK) signaling pathway and starch and sucrose metabolism (Fig. 7D). Combined with gene annotation, we

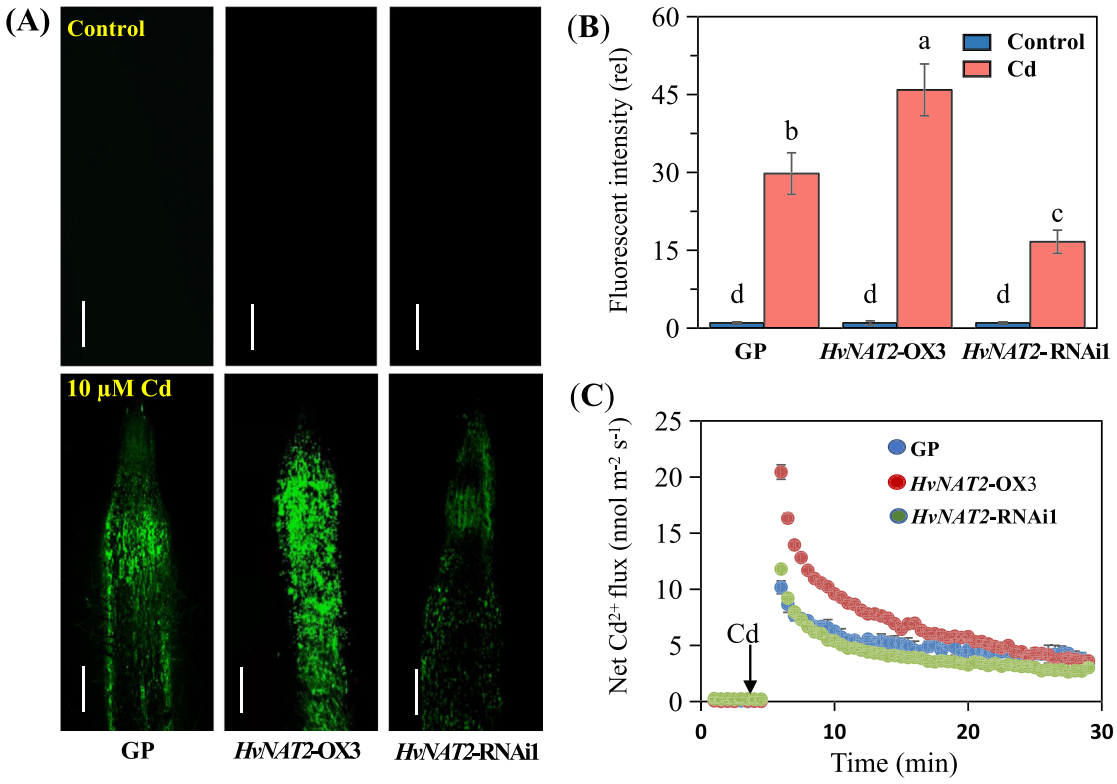

Fig. 5. Cd distribution and ion fluxes of *HvNAT2*-OX3 and *HvNAT2*-RNAi1 plants under control and Cd stress conditions. (A) The binding of Cd^{2+} to Leadamium™ Green AM dye at longitudinal section of roots. Plants were exposed to 0 and 10 μM Cd for 15 days before staining with Leadamium™ Green AM. Scale bars = 300 μm. (B) Cd^{2+} fluorescence density. (C) Transient and steady-state changes in Cd^{2+} fluxes from root epidermal cells of plants exposed to 10 μM Cd. Data are means ± SD of three biological replicates and different letters stand for significantly different at $p \leq 0.05$.

found that contrasting expression levels of DEGs involved in redox (e.g. *GSTs, GPXs, AOX, AAO*), MAPK signaling, ethylene signaling and membrane transport (e.g. *HMA3, ERD4, ACA*) in the OX lines in comparison to GP. Moreover, qRT-PCR detection of 26 differentially expressed genes corroborated the above sequencing results (Table 1; Fig. S7). For instance, both RNA-seq and qRT-PCR demonstrated that transcripts of three *GPXs* showed no difference in the OX lines than in GP under control conditions, but Cd stress significantly upregulated these DEGs in the OX lines compared to GP (Table 1; Fig. S7). These results indicated that improving antioxidant capacity may be an important way for the OX lines to become Cd tolerant.

Therefore, we tested the antioxidant capacity by measuring enzyme activities of SOD, GPX, APX, GST and POD as well as production of GSH, MDA and NO in both roots and shoots of the OX lines and in WT GP (Fig. 8). We showed that Cd stress results in an increase in SOD, POD, GPX and APX activities of *HvNAT2*-OX lines in shoots, which was significantly higher than that of GP (Fig. 8A-E). Also, POD, GPX and APX activities were higher in OX lines than GP after Cd treatment (Fig. 8A-E). Although Cd stress did not cause an increase of GST activity, the OX lines showed higher GST activities both in control and Cd conditions (Fig. 8D). Under Cd stress, the *HvNAT2*-OX lines had higher GSH contents compared with GP (Fig. 8F). The MDA content in the shoots and roots of GP was increased by 74.8% and 95.3% under Cd stress over the control, respectively; the corresponding values in the *HvNAT2*-OX line were reduced to 49.2% and 54.1% (Fig. 8G). Overexpression of *HvNAT2* showed little effect on NO content in shoots, but the roots of *HvNAT2*-OX lines showed significantly higher Cd-induced increases in NO content compared with GP (Fig. 8H).

Discussion

miRNA-seq profiling reveals key miRNAs in Cd-tolerant barley genotypes

As key regulators in the growth and development of plants, miRNAs can specifically bind to the target mRNAs and affect gene expression [37]. Previous reports suggest that miRNAs in plants are associated with abiotic stress responses like drought, cold, salt in *Arabidopsis* [38], *Oryza sativa* [39], *Glycine* max [40], *Z. mays* [41], and *Triticum aestivum* [42]. In addition, miRNAs are also widely involved in responses to heavy metal stress. Gu et al. [43] found that miR398 regulates the *copper-zinc superoxide dismutase* (*CuZn-SOD*) gene to restore redox balance to enhance Cd tolerance. In *Arabidopsis*, Cd induces the expression of miRNA172b-5p, miRNA172e-5p, and miRNA472-3p, which reduce the expression of their target gene, *mutS homolog 6* (*MSH6*), to enhance the recognition and repair of Cd-induced DNA damage [44]. In poplar (*Populus balsamifera* L.), miR395 and miR399 are reported to affect Cd accumulation by regulating *ATP sulfurylase 3* (*ATPS3*) [45].

Here, we identified 17 Cd-tolerance-associated miRNAs differentially expressed in two barley genotypes differing in Cd tolerance and accumulation, showing a complex and dynamic gene regulatory network (Fig. 1B). Among these miRNAs, the target gene predicted for miR156g-3p_3 was identified as a nucleobase-ascorbate transporter (Fig. 1C; Tables S6). Recent research has demonstrated that the up-regulation of CAT and POD activities in *MdNAT* overexpression plants was significantly higher than WT apple plants under salt stress. Also, salt-tolerance-related gene expression was increased along with a decreased Na^+/K^+ ratio, which alleviates the toxic effect of Na^+ in transgenic apple plants

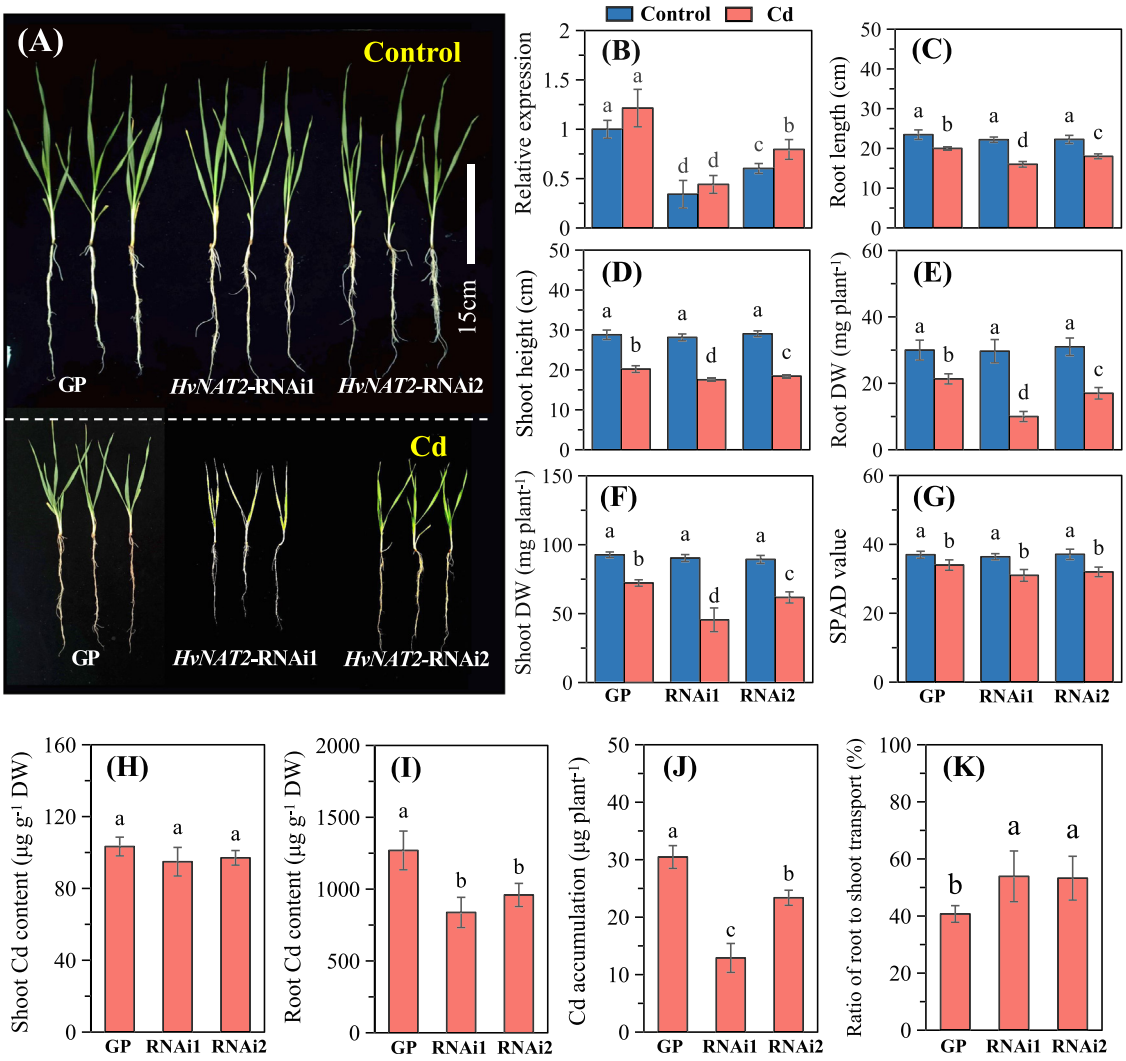

Fig. 6. Functional assessment of *HvNAT2 via* gene silencing in barley. (A) Phenotype of GP and *HvNAT2*-RNAi lines (RNAi1, RNAi2) under control and Cd stress conditions. (B) Relative expression of *HvNAT2* in GP and *HvNAT2*-RNAi lines. (C-G) Root length (C), Shoot height (D), root dry weight (E), shoot dry weight (F), and relative chlorophyll content (SPAD) (G) of GP and *HvNAT2*-RNAi lines. (H-K) Shoot Cd concentration (H), root Cd concentration (I), Cd accumulation (J) and ratio of root to shoot transport (K) of GP and *HvNAT2*-RNAi lines. Plants were exposed to 10 μM Cd for 15 days. All data are means ± SD of three biological replicates and different letters stand for significantly different at $p \leq 0.05$.

[23]. Under drought stress, overexpression of *MdNAT7* increased the chlorophyll content and antioxidant enzyme activity [23]. Therefore, *HvNAT2* may be important in barley to increase the antioxidant capacity under Cd stress under the regulation of miR156g-3p_3. Therefore, we suggest that *HvNAT2* is a novel candidate gene contributing to Cd tolerance in barley.

NAT2s are evolutionarily conserved for growth and stress response in plants

The NAT family was discovered by cloning the *UraA* and *PyrP* uracil permeases of *Escherichia coli* [46] and *Bacillus subtilis* [47], and the *UapA* and *UapC* uric acid-xanthine permeases of *Aspergillus nidulans* [48]. NAT proteins have been found in many plants, including *A. thaliana* [20], *O. sativa* [49], *Z. mays* [19], *M. pumila* [22,24]. In addition, NATs also exist in mammals where they mediate the transport of L-ascorbic acid, a key antioxidant [50]. This is related to the distinctive motif [Q/E/P]-NXGXXXXT-[R/K/G] and the QH motif of NAT proteins; both of them are involved in substrate recognition and transportation [51]. In the motif [Q/E/P]-NXGXXXXT-[R/K/G], the first amino acid in the nucleobase transporters motif is Q/E, while it is P in the ascorbate transporters [52].

In this study, NAT2 exists in evolutionarily multifarious organisms ranging from green algae to angiosperms (Fig. 2B). Based on the signature motif, green plant NAT2 has probably evolved from streptophyte algae with E as the first amino acid in the motif [Q/E/P]-NXGXXXXT-[R/K/G], which was evolutionary conserved across the species in the major lineages of land plants examined including barley. The first amino acid is Q and a few amino acid residues are not conserved in red algae such as *Gracilaria chouae* and *Desmarestia viridis* as compared to those in green plants (Fig. 2D). Moreover, studies showed that loss function of the NAT protein, ZmLPE1, in maize caused a defective chloroplast phenotype [18], and NAT proteins play roles in long-distance metabolite redistribution in *Arabidopsis* [20]. Interestingly, NAT proteins in *M. pumila* responded to salt and drought stress; MdNAT1 and MdNAT7 were shown to regulate drought and salt tolerance [23]. Therefore, we suggested that NAT2 is conserved in plants encoding transporter with important functions in plant growth and adaptation to abiotic stresses. Further study is required to better understand the molecular evolution, physiological changes and

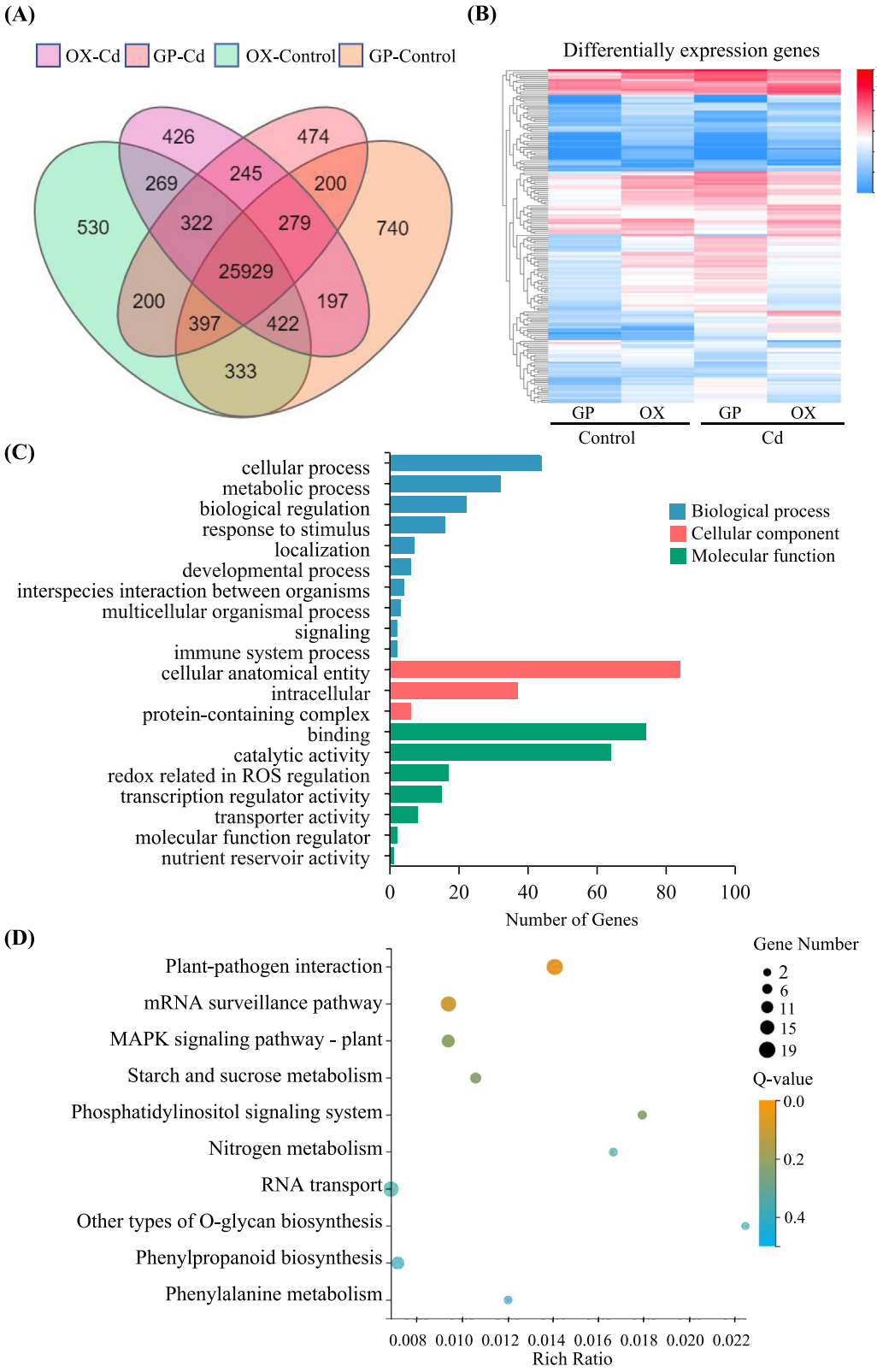

Fig. 7. Transcriptomics analysis of *HvNAT2*-OX lines. (A) Gene expression in four libraries (GP-Control, GP-Cd, OX-Control, OX-Cd). (B) Cluster analysis of 173 differently expressed genes compared the OX-lines to GP. (C, D) GO (C) and KEGG (D) analysis of differently expressed genes between *HvNAT2*-OX lines and GP. GP, Golden Promise; OX: *HvNAT2*-OX lines; GO, Gene Ontology; KEGG, Kyoto Encyclopedia of Genes and Genomes.

Table 1
Key differentially expressed genes in *HvNAT2*-OX and GP under the control and Cd.

Gene ID	Fold change (OX vs GP)				Predicted molecular function
	RNA-seq		qRT-PCR		
	Control	Cd	Control	Cd	
HORVU3Hr1G073180	4.19	4.54	5.81	6.44	Nucleobase-ascorbate transporter 2 (NAT2) contributes to Cd tolerance in barley in this study
HORVU1Hr1G057630	−0.18	1.38	−0.07	1.55	CSC1-like protein (ERD4) for hyperosmolarity-gated non-selective cation channel that permeates Ca^{2+} and potentially Cd^{2+} ions
HORVU0Hr1G020790	−0.31	1.04	0.33	1.05	Calcium-transporting ATPase 9 (ACA9) permeates Ca^{2+} and potentially Cd^{2+} ions
HORVU7Hr1G097210	−0.14	1.00	−0.33	1.20	Cadmium/zinc-transporting ATPase 3 (HMA3) for Cd homeostasis
HORVU1Hr1G043470	3.56	2.91	8.29	7.56	Glutathione S-transferase T3 (GST3) for oxidative stress response
HORVU2Hr1G018440	−0.39	1.14	−0.02	1.10	Glutathione Peroxidase 2 (GPX2) protects against oxidative stresses
HORVU2Hr1G044360	−0.3	1.03	−0.07	1.36	Glutathione Peroxidase 2 (GPX2) protects against oxidative stresses
HORVU3Hr1G024510	−0.19	1.29	−0.33	1.19	Glutathione Peroxidase 25 (GPX25) protects against oxidative stresses
HORVU6Hr1G090560	−0.09	1.29	−0.66	1.22	Glutathione S-transferase isoform X2 (GSTU6) for toxin catabolic process
HORVU3Hr1G099080	−0.45	1.14	−0.82	1.38	Glutaredoxin-C2 (GRXC6) for cellular response to oxidative stress
HORVU7Hr1G087250	−0.53	1.39	0.41	1.04	L-ascorbate oxidase-like (AAO) in redox system of oxidative stress
HORVU6Hr1G026820	3.85	3.63	2.58	2.34	Thioredoxin-like protein (Trx) participates as a hydrogen donor in redox reactions
HORVU6Hr1G065430	0.99	1.67	0.25	1.81	Ethylene-responsive transcription factor 27-like (ERF027) acts as the components of stress signal transduction pathways
HORVU2Hr1G004200	−0.34	1.6	−0.51	1.59	1-aminocyclopropane-1-carboxylate oxidase homolog 1-like (ACO1) for Ethylene biosynthesis, Plant defense
HORVU2Hr1G108180	0.19	1.19	0.22	1.39	Anthocyanidin reductase ((2S)-flavan-3-ol-forming)-like isoform X2 (ANRX2) with oxidoreductase activity
HORVU0Hr1G005420	1.36	−1.03	1.24	−0.68	Alternative oxidase (AOX) controls the synthesis of ROS and NO
HORVU2Hr1G101990	1.83	−0.88	1.37	−0.70	Alternative oxidase 1a (AOX1a) controls the synthesis of ROS and NO
BGI_novel_G000483	2.1	−1.93	2.11	−1.15	Phenylalanine ammonia-lyase (PAL) in response to oxidative stress
HORVU5Hr1G093700	0.6	1.08	−0.68	1.07	Linoleate 9S-lipoxygenase 3 (LOX3) in the pathway of fatty acid metabolism and in Lipid metabolism
HORVU4Hr1G066270	0.49	1.16	0.25	1.59	Allene oxide synthase 2 (AOS3) in the pathway of fatty acid metabolism and in lipid metabolism
HORVU5Hr1G059310	4.16	3.53	7.5	6.75	Glutathione gamma-glutamylcysteinyltransferase 1 (PCS1) for phytochelatins and homophytochelatins for heavy metal binding
HORVU6Hr1G036920	0.31	1.39	0.21	1.25	Cytokinin-O-glucosyltransferase 3 for cellular detoxification
HORVU7Hr1G113830	0.79	1.04	0.15	2.09	WRKY transcription factor 2 in the pathway of MAPK signaling
HORVU7Hr1G057410	−0.75	1.09	−0.43	1.27	R2R3 MYB transcriptional factor (MYB) may involve in stress regulation
HORVU2Hr1G010030	2.65	2.41	3.12	1.41	Arginine decarboxylase 2 (ADC2) in the pathway of arginine metabolism
HORVU4Hr1G085450	4.67	5.04	7.31	8.56	MADS-box transcription factor 51 (MADS51) may involve in stress regulation

List of redox related genes in ROS regulation, and signaling, transport related genes differentially expressed in *HvNAT2*-OX *vs* GP plants. Fold change (OX ***vs*** GP) is $\log_2$N, $\log_2 N \geq 1$ are up-regulated, between $0 < |\log_2 N| < 1$ are unchanged and $\log_2 N \leq -1$ are down-regulated, Q-value ≤ 0.001. The Predicted Molecular Function is obtained from https://www.uniprot.org/. The qRT-PCR of genes: an additional hydroponic experiment was carried out again using GP and *HvNAT2*-OX lines under control and 10 μM Cd treatment with three replicates. Total RNA was isolated from leaves of barley plants after 24 h of Cd treatment using TRIzol reagent (Invitrogen, Karlsruhe, Germany). qRT–PCR reaction was performed on LightCycler 480 System (Roche, Germany). All primers used are listed in Tables S2. GAPDH was used as internal control.

selectivity of NAT2 to different substrates in a range of evolutionarily important plant species in addition to *Arabidopsis* and a few crop species.

HvNAT2 enhances Cd tolerance in barley by improving antioxidative capacity

So far, no NAT in plants have been reported to have important function related to Cd stress. In this study, the expression of *HvNAT2* showed a rapid response to Cd (Fig. 3A). Overexpression of *HvNAT2* improved Cd tolerance (Fig. 4) and distinctively regulated the transcriptome of *HvNAT2* OX lines (Fig. 7; Table 1; Table S11), indicating a role of *HvNAT2* resist to Cd detriment in barley. Most notably, we demonstrated that overexpression of *HvNAT2* improved the antioxidant capacity at both the transcript and enzyme levels in barley.

Under stress conditions, H_2O_2 is reduced by GSH, and GSH is oxidized to GSSG by GPX, and GSSG is reduced to GSH by GR, forming a redox cycle to eliminate ROS [53]. Roxas et al. [54] found that overexpression of *GST* in tobacco improved the plant's ability to resist stress and increased the ability to eliminate peroxides with GSH. The Trx-TrxR system constitutes another set of intracellular processes to eliminate ROS and interacts with other redox systems [55]. The removal of hydrogen peroxide during photosynthesis by Trx is also related to the Prx system [56]. In the 173Cd-induced DEGs in both OX lines and GP, 17 DEGs were involved in redox related in ROS regulation, which form the largest group of DEGs given the close genetic relationship between OX line and GP (Tables 1, S11). Here, the Cd-induced expression of *GST, GPXs*, and *Trx* were upregulated in *HvNAT2*-OX lines compared with GP, which increased GSH contents and thus enhances the ROS scavenging capacity in the OX lines. Moreover, *HvNAT2*-OX lines exhibited significantly higher SOD, GPX, APX, GST and POD activities and GSH contents with less MDA accumulation in response to Cd stress compared with GP (Fig. 8).

Arginine is a precursor to synthesis of polyamine (PA) and NO. Arginine decarboxylase (ADC) and nitrous oxide synthase (NOS) are the key enzymes that determine the direction of arginine metabolism [57,58]. PA accumulation is important for abiotic stress tolerance [59] and increases in endogenous and exogenous PA have been shown to confer abiotic stress tolerance through the regulation of antioxidant machineries [60,61]. Overexpression of *spermidine synthase 1* (*SPDS1*) in pear (*Pyrus communis* L.) led to the activation of antioxidant enzymes, resulting in increased tolerance to heavy metals [62]. Ectopic expression of *PtADC* of *Citrus* (*Poncirus*) *trifoliata* L. increased tolerance to dehydration and drought, with a concurrent, large inhibition of ROS generation [61]. We found that the higher expression of *ADC* in the *HvNAT2*-OX lines potentially promotes the synthesis of PAs thereby enhancing antioxidant capacity. In addition, the expression of ADC is associated with MAPK and many transcription factors. Huang et al. [63] reported that the expression of *NtADC1* and *NtSAMDC* (S-adenosylmethionine decarboxylase) was induced in PtrMAPK overexpressing plants. Transcription factors like WRKY (*FcWRKY70*)

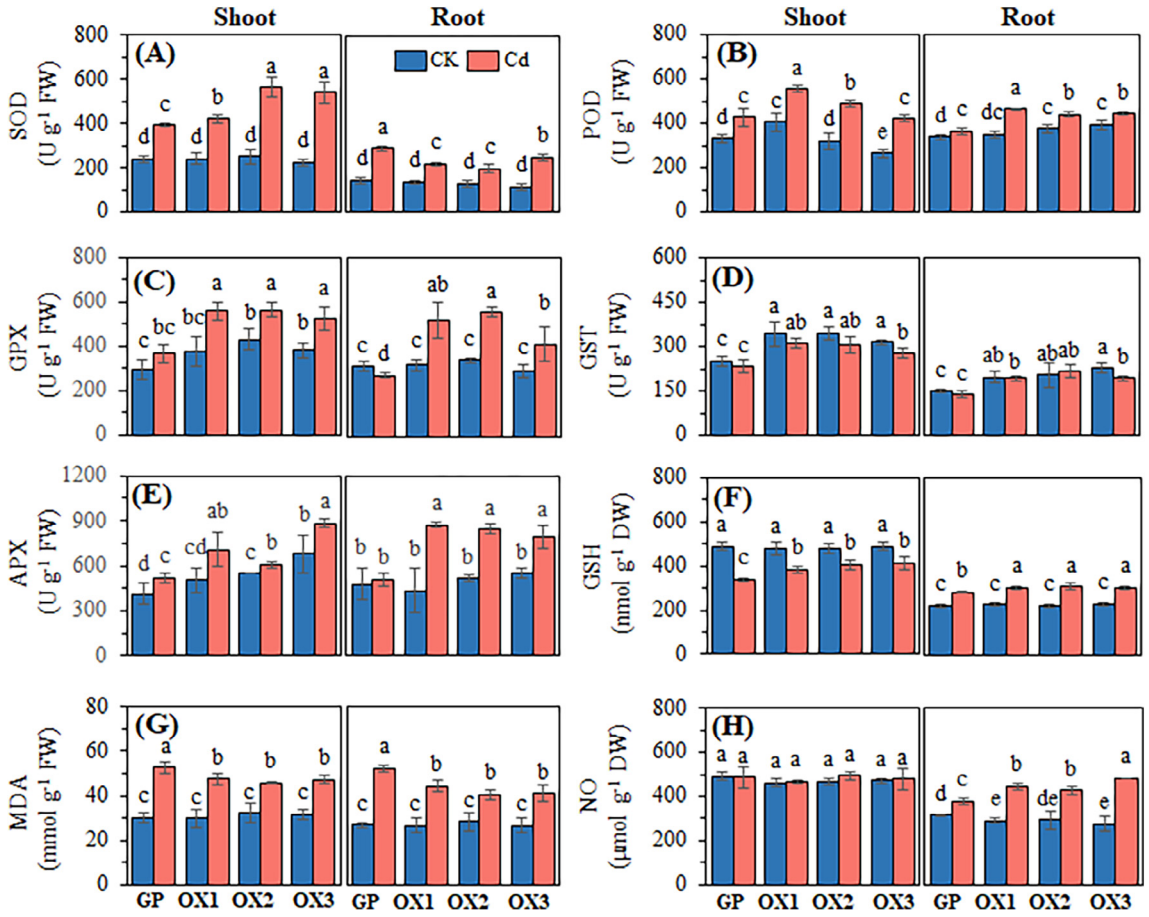

Fig. 8. Antioxidant capacity assessment of *HvNAT2*-OX lines (OX1, OX2, OX3) and GP under control and Cd stress conditions. (A-H) Activities of SOD (A), POD (B), GPX (C), GST (D), APX (E) and contents of GSH (F), MDA (G), NO (H) in the shoots and roots of plants exposed to 0 or 10 μM Cd. Data are means ± SD of three biological replicates and different letters stand for significantly different at $p \leq 0.05$.

and MYB (*PtsrMYB*, *GbMYB5*) have been reported to be positive regulators of ADC expression for putrescine (Put) synthesis under abiotic stresses [64–66].

Signal transduction is important in responses to abiotic stress [67–69]. Here, the Cd-induced transcriptome of GP and *HvNAT2*-OX lines revealed that overexpression of *HvNAT2* activates MAPK and ethylene signaling. MAPK cascades are ubiquitous signal transduction pathway in plants, playing essential roles in transmitting abiotic stress signals and enhancing plant defense mechanisms [70]. The WRKY family is a class of transcription factors that receive signals in MAPK signaling pathway, thus regulating the expression of genes participating in plant responses to abiotic stresses. For instance, OsMAPK3 can phosphorylate the SP site of OsWRKY30 and improve the drought tolerance of plants [71–73]. In addition, AtMAPK6 and AtMAPK3 can phosphorylate AtWRKY33, thereby enhancing the expression of 1-*aminocyclopropane-1-carboxylic acid synthase* (*AtACS2*) and *AtACS6* to promote ethylene synthesis [74]. Under oxidative stress, AtMAPK6 can phosphorylate the ethylene response factor, ERF6, promoting its binding to the ROS response element, the ROSE7/GCC box, thereby regulating the transcription of ROS responsive genes [75]. Taken together, the up-regulation of *ACO* and *ERF* related to ethylene synthesis and MAPK pathway in *HvNAT2*-OX lines indicated that the *HvNAT2*-mediated activation of MAPK and ethylene signaling may participate in the maintenance of redox and ROS scavenging. However, the activation of MAPK pathway by overexpression of *HvNAT2* remains to be explored in the future.

Does HvNAT2 indirectly regulate Cd transport?

The accumulation of heavy metals such as Cd in plants is related to the absorption by roots from the soil, the transport from the roots to the vascular system and the transfer and storage from the roots to the aboveground tissues [69]. Among the key heavy metal transporters, HMA is a subfamily of P-type-ATPases that transport Zn^{2+} and Cd^{2+}. Tonoplast localized HMA3 plays a significant role in the detoxification of heavy metals in plants by sequestrating toxic heavy metals into the vacuole [76–78]. For instance, overexpression of *OsHMA3* in rice causes more Cd to be transported to the vacuoles of root cells, thus limiting the translocation of Cd from roots to shoots while increasing the Cd content in the roots. This results in a decrease in Cd concentration and an increase in Cd tolerance in leaves and grains [79]. In *Sedum plumbizincicola*, overexpression of *SpHMA3* did not change the distribution pattern of Cd, but significantly increased the concentration of Cd in roots and shoots [80]. In this study, *HvHMA3* was significantly up-regulated in *HvNAT2*-OX lines compared with GP under Cd treatment (Table S11; Fig. S8). It is unlikely that HvNAT2 interacts directly with HvHMA3 to enhance its expression, because both of them are membrane transporter proteins. Thus, one possibility may be that *HvNAT2*-OX lines had higher antioxidative capacity, allowing more Cd to be accumulated in roots and shoot compared to GP. The accumulation of more Cd in vacuoles requires a higher expression of *HvHMA3* in *HvNAT2*-OX lines. Moreover, the hyperosmolarity-gated, non-selective cation channel, CSC1-like

protein (ERD4) was significantly up-regulated by Cd in *HvNAT2*-OX lines, which partially explains the higher Cd accumulation because this channel may allow both Ca^{2+} and Cd^{2+} influx into root cells. In summary, *HvNAT2*-OX lines exhibited better membrane transport capacity compared to GP causing higher Cd accumulation and enhanced Cd tolerance. This property may play a very important role in phytoremediation.

Conclusion

We reported that miR156g-3p_3 targeted a novel NAT gene, *HvNAT2*, that has been functionally characterized to determine its role in Cd tolerance in barley. Overexpression of *HvNAT2* enhanced Cd tolerance, with OX plants showing higher antioxidant gene expression, ROS enzyme activities and GSH contents. Transcriptomic analysis revealed that enhanced antioxidant capacity is due to activation of MAPK and ethylene signaling pathways, increased polyamine synthesis, and enhanced activity of the GSH-GSSG cycle. Therefore, given the high evolutionary conservation of *NAT2*, genetic engineering of NAT in plants and green algae may have potential in the remediation of soil and water Cd pollution, to provide safer and cleaner soil environment for food production.

Compliance with Ethics Requirement

This article does not contain any studies with human or animal subjects.

The authors declare that they have no known competing financial interests or personal relationships that could have influenced the work reported in this paper.

CRediT authorship contribution statement

Nianhong Wang: Methodology, Validation, Formal analysis, Investigation, Data curation, Writing – original draft. **Xueyi Zhou:** Validation, Investigation. **Shouheng Shi:** Investigation. **Shuo Zhang:** Investigation. **Zhonghua Chen:** Formal analysis, Writing – original draft, Writing – review & editing. **Mohamed Abdelalim Ali:** Writing – review & editing. **Imrul Mosaddek Ahmed:** Writing – review & editing. **Yizhou Wang:** Writing – review & editing. **Feibo Wu:** Conceptualization, Methodology, Resources, Formal analysis, Writing – original draft, Writing – review & editing, Supervision, Project administration, Funding acquisition.

Declaration of Competing Interest

The authors declare that they have no known competing financial interests or personal relationships that could have appeared to influence the work reported in this paper.

Acknowledgements

The authors sincerely thank Prof. Paul Holford from Western Sydney University for his constructive suggestions and amendments in writing this paper. We are thanks for the financial support from the National Natural Science Foundation of China (Major NSFC-ASRT International Joint Research Project 3211101286) and the Key Research Foundation of Science and Technology Department of Zhejiang Province of China (2021C02064-3, 2016C02050-9-7).

Appendix A. Supplementary data

Supplementary data to this article can be found online at https://doi.org/10.1016/j.jare.2022.04.001.

References

[1] Järup L, Åkesson A. Current status of cadmium as an environmental health problem. Toxicol Appl Pharmacol 2009;238(3):201–8.
[2] Khan MA, Khan S, Khan A, Alam M. Soil contamination with cadmium, consequences and remediation using organic amendments. Sci Total Environ 2017;601-602:1591–605.
[3] Tang B, Luo M, Zhang Y, Guo H, Li J, Song W, et al. Natural variations in the P-type ATPase heavy metal transporter gene ZmHMA3 control cadmium accumulation in maize grains. J Exp Bot 2021;72(18):6230–46.
[4] Cao F, Wang R, Cheng W, Zeng F, Ahmed IM, Hu X, et al. Genotypic and environmental variation in cadmium, chromium, lead and copper in rice and approaches for reducing the accumulation. Sci Total Environ 2014;496:275–81.
[5] Cao F, Chen F, Sun H, Zhang G, Chen Z, Wu F. Genome-wide transcriptome and functional analysis of two contrasting genotypes reveals key genes for cadmium tolerance in barley. BMC Genomics 2014;15:1–14.
[6] Wang X, Gong X, Cao F, Wang Y, Zhang G, Wu F. HvPAA1 encodes a P-Type ATPase, a novel gene for cadmium accumulation and tolerance in barley (*Hordeum vulgare* L.). Int J Mol Sci 2019;20:1732.
[7] Andresen E, Küpper H. Cadmium toxicity in plants. Cadmium from Toxic to Essentiality 2013:395–413.
[8] Shahid M, Dumat C, Khalid S, Niazi NK, Antunes PMC. Cadmium bioavailability, uptake, toxicity and detoxification in soil-plant system. Rev Environ Contam Toxicol 2016;241:73–137.
[9] Rono JK, Le Wang L, Wu X, Cao H, Zhao Y, Khan IU, et al. Identification of a new function of metallothionein-like gene OsMT1e for cadmium detoxification and potential phytoremediation. Chemosphere 2021;265:129136.
[10] Kumar S, Asif MH, Chakrabarty D, Tripathi RD, Dubey RS, Trivedi PK. Expression of a rice Lambda class of glutathione S-transferase, OsGSTL2, in *Arabidopsis* provides tolerance to heavy metal and other abiotic stresses. J Hazard Mater 2013;248-249:228–37.
[11] Le Martret B, Poage M, Shiel K, Nugent GD, Dix PJ. Tobacco chloroplast transformants expressing genes encoding dehydroascorbate reductase, glutathione reductase, and glutathione-S-transferase, exhibit altered anti-oxidant metabolism and improved abiotic stress tolerance. Plant Biotechnol J 2011;9(6):661–73.
[12] Qiao K, Gong L, Tian Y, Wang H, Chai T. The metal-binding domain of wheat heavy metal ATPase 2 (TaHMA2) is involved in zinc/cadmium tolerance and translocation in *Arabidopsis*. Plant Cell Rep 2018;37(9):1343–52.
[13] Verret F, Gravot A, Auroy P, Leonhardt N, David P, Nussaume L, et al. Overexpression of AtHMA4 enhances root-to-shoot translocation of zinc and cadmium and plant metal tolerance. FEBS Lett 2004;576(3):306–12.
[14] Courbot M, Willems G, Motte P, Arvidsson S, Roosens N, Saumitou-Laprade P, et al. A major quantitative trait locus for cadmium tolerance in *Arabidopsis* halleri colocalizes with HMA4, a gene encoding a heavy metal ATPase. Plant Physiol 2007;144(2):1052–65.
[15] Morel Mélanie, Crouzet Jérôme, Gravot A, Auroy P, Leonhardt N, Vavasseur A, et al. AtHMA3, a P1B-ATPase allowing Cd/Zn/co/Pb vacuolar storage in *Arabidopsis*. Plant Physiol 2009;149(2):894–904.
[16] Baliardini C, Meyer C-L, Salis P, Saumitou-Laprade P, Verbruggen N. CATION EXCHANGER1 cosegregates with cadmium tolerance in the metal hyperaccumulator *Arabidopsis* halleri and plays a role in limiting oxidative stress in *Arabidopsis* Spp. Plant Physiol 2015;169(1):549–59.
[17] Sun H, Chen Z, Chen F, Xie L, Zhang G, Vincze E, et al. DNA microarray revealed and RNAi plants confirmed key genes conferring low Cd accumulation in barley grains. BMC Plant Biol 2015;15:1–17.
[18] Schultes NP, Brutnell TP, Allen A, Dellaporta SL, Nelson T, Chen J. Leaf permease1 gene of maize is required for chloroplast development. Plant Cell 1996;8:463–75.
[19] Argyrou E, Sophianopoulou V, Schultes N, Diallinas G. Functional characterization of a maize purine transporter by expression in *Aspergillus nidulans*. Plant Cell 2001;13(4):953–64.
[20] Maurino VG, Grube E, Zielinski J, Schild A, Fischer K, Flügge U-I. Identification and expression analysis of twelve members of the nucleobase–ascorbate transporter (NAT) gene family in Arabidopsis thaliana. Plant Cell Physiol 2006;47(10):1381–93.
[21] Cai X, Ye J, Hu T, Zhang Y, Ye Z, Li H. Genome-wide classification and expression analysis of nucleobase–ascorbate transporter (NAT) gene family in tomato. Plant Growth Regul 2014;73(1):19–30.
[22] Sun T, Jia D, Huang L, Shao Y, Ma F. Comprehensive genomic identification and expression analysis of the nucleobase-ascorbate transporter (NAT) gene family in apple. Sci Hortic 2016;198:473–81.
[23] Sun T. Functional analysis of MdNAT1 and MdNAT7 transporters in Malus under drought and salinity stresses. Shanxi China: Northwest Agric. For. Univ; 2018. PhD thesis.
[24] Sun T, Pei T, Yang L, Zhang Z, Li M, Liu Y, et al. Exogenous application of xanthine and uric acid and nucleobase-ascorbate transporter MdNAT7 expression regulate salinity tolerance in apple. BMC Plant Biol 2021;21:1–14.

[25] Hayes P, Carrijo D, Meints B. Towards low cadmium accumulation in barley. Nat Food 2020;1:465.
[26] Lei GJ, Fujii-Kashino M, Wu DZ, Hisano H, Saisho D, Deng F, et al. Breeding for low cadmium barley by introgression of a Sukkula-like transposable element. Nat Food 2020;1(8):489–99.
[27] Chen F, Wu F, Dong J, Vincze E, Zhang G, Wang F, et al. Cadmium translocation and accumulation in developing barley grains. Planta 2007;227(1):223–32.
[28] Wu F, Zhang G, Dominy P. Four barley genotypes respond differently to cadmium: lipid peroxidation and activities of antioxidant capacity. Environ Exp Bot 2003;50:67–78.
[29] Qiu C, Liu L, Feng X, Hao P, He X, Cao F, et al. Genome-wide identification and characterization of drought stress responsive microRNAs in tibetan wild barley. Int J Mol Sci 2020;21:2795.
[30] Feng X, Liu W, Qiu C-W, Zeng F, Wang Y, Zhang G, et al. HvAKT2 and HvHAK1 confer drought tolerance in barley through enhanced leaf mesophyll H^+ homoeostasis. Plant Biotechnol J 2020;18(8):1683–96.
[31] Leebens-Mack JH, Barker MS, Carpenter EJ, Deyholos MK, Gitzendanner MA, Graham SW, et al. One thousand plant transcriptomes and the phylogenomics of green plants. Nature 2019;574:679–85.
[32] Shen Q, Fu L, Su T, Ye L, Huang Lu, Kuang L, et al. Calmodulin HvCaM1 negatively regulates salt tolerance via modulation of HvHKT1s and HvCAMTA4. Plant Physiol 2020;183(4):1650–62.
[33] Chen F, Wang F, Sun H, Cai Y, Mao W, Zhang G, et al. Genotype-dependent effect of exogenous nitric oxide on Cd-induced changes in antioxidative metabolism, ultrastructure, and photosynthetic performance in barley seedlings (*Hordeum vulgare*). J Plant Growth Regul 2010;29(4):394–408.
[34] Chen F, Wang F, Wu F, Mao W, Zhang G, Zhou M. Modulation of exogenous glutathione in antioxidant defense system against Cd stress in the two barley genotypes differing in Cd tolerance. Plant Physiol Biochem 2010;48 (8):663–72.
[35] Mak M, Zhang M, Randall D, Holford P, Milham P, Wu F, et al. Chloride transport at plant-soil Interface modulates barley cd tolerance. Plant Soil 2019;441(1-2):409–21.
[36] Pineros MA, Shaff JE, Kochian LV. Development, characterization, and application of a cadmium-selective microelectrode for the measurement of cadmium fluxes in roots of Thlaspi species and wheat. Plant Physiol 1998;116:1393–401.
[37] Shriram V, Kumar V, Devarumath RM, Khare TS, Wani SH. MicroRNAs as potential targets for abiotic stress tolerance in plants. Front Plant Sci 2016;7:817.
[38] Barciszewska-Pacak M, Milanowska K, Knop K, Bielewicz D, Nuc P, Plewka P, et al. Arabidopsis microRNA expression regulation in a wide range of abiotic stress responses. Front Plant Sci 2015;6:410.
[39] Goswami K, Tripathi A, Sanan-Mishra N. Comparative miRomics of salt-tolerant and salt-sensitive rice. J Integr Bioinform 2017;14:20170002.
[40] Sun Z, Wang Y, Mou F, Tian Y, Chen L, Zhang S, et al. Genome-wide small RNA analysis of soybean reveals auxin-responsive microRNAs that are differentially expressed in response to salt stress in root apex. Front Plant Sci 2016;6:1273.
[41] Upadhyay U, Singh P, Verma OP. Role of microRNAs in regulating drought stress tolerance in maize. J Pharmacogn Phytochem 2019;8:328–31.
[42] Uzma, Iftikhar H, Ghori Z, Ali SH, Sheikh S, Gul A, Wheat responses to stress and biotechnological approaches for improvement. In: Hasanuzzaman M, Nahar K, Hossain M, eds. Wheat Production in Changing Environments. Singapore: Springer, Singapore; 2019. p. 343–392.
[43] Gu Q, Chen Z, Yu X, Cui W, Pan J, Zhao G, et al. Melatonin confers plant tolerance against cadmium stress via the decrease of cadmium accumulation and reestablishment of microRNA-mediated redox homeostasis. Plant Sci 2017;261:28–37.
[44] Wang H, Cao Q, Zhao Q, Arfan M, Liu W. Mechanisms used by DNA MMR system to cope with Cadmium-induced DNA damage in plants. Chemosphere 2020;246:125614.
[45] Shi W, Liu W, Ma C, Zhang Y, Ding S, Yu W, et al. Dissecting microRNA–mRNA regulatory networks underlying sulfur assimilation and cadmium accumulation in Poplar leaves. Plant Cell Physiol 2020;61(9):1614–30.
[46] Andersen PS, Frees D, Fast R, Mygind B. Uracil uptake in Escherichia coli K-12: isolation of uraA mutants and cloning of the gene. J Bacteriol 1995;177:2008–13.
[47] Turner RJ, Lu Y, Switzer RL. Regulation of the Bacillus subtilis pyrimidine biosynthetic (pyr) gene cluster by an autogenous transcriptional attenuation mechanism. J Bacteriol 1994;176(12):3708–22.
[48] Diallinas D, Gorfinkiel G, Arst HN, Cecchetto C, Scazzocchio S. Genetic and molecular characterization of a gene encoding a wide specificity purine permease of *Aspergillus nidulans* reveals a novel family of transporters conserved in prokaryotes and eukaryotes. J Biol Chem 1995;270(15):8610–22.
[49] Yu J, Hu S, Wang J, Wong G-S, Li S, Liu B, et al. A draft sequence of the rice genome (*Oryza sativa* L. ssp. indica). Science 2002;296(5565):79–92.
[50] Bürzle M, Suzuki Y, Ackermann D, Miyazaki H, Maeda N, Clémençon B, et al. The sodium-dependent ascorbic acid transporter family SLC23. Mol Aspects Med 2013;34(2-3):436–54.
[51] Pantazopoulou A, Diallinas G. The first transmembrane segment (TMS1) of UapA contains determinants necessary for expression in the plasma membrane and purine transport. Mol Membr Biol 2006;23(4):337–48.
[52] Gournas C, Papageorgiou I, Diallinas G. The nucleobase–ascorbate transporter (NAT) family: genomics, evolution, structure–function relationships and physiological role. Mol Biosyst 2008;4:404–16.
[53] Wrzaczek M, Brosché M, Kangasjärvi J. ROS signaling loops—production, perception, regulation. Curr Opin Plant Biol 2013;16(5):575–82.
[54] Roxas VP, Lodhi SA, Garrett DK, Mahan JR, Allen RD. Stress tolerance in transgenic tobacco seedlings that overexpress glutathione S-transferase/ glutathione peroxidase. Plant Cell Physiol 2000;41(11):1229–34.
[55] Xu W, Ngo L, Perez G, Dokmanovic M, Marks PA. Intrinsic apoptotic and thioredoxin pathways in human prostate cancer cell response to histone deacetylase inhibitor. Proc Natl Acad Sci 2006;103(42):15540–5.
[56] Meyer Y, Belin C, Delorme-Hinoux V, Reichheld JP, Riondet C. Thioredoxin and glutaredoxin systems in plants: molecular mechanisms, crosstalks, and functional significance. Antioxid Redox Signal 2012;17:1124–60.
[57] Piacenza L, Peluffo G, Radi R. L-arginine-dependent suppression of apoptosis in Trypanosoma cruzi: contribution of the nitric oxide and polyamine pathways. Proc Natl Acad Sci 2001;98:7301–6.
[58] Lamattina L, García-Mata C, Graziano M, Pagnussat G. Nitric oxide: the versatility of an extensive signal molecule. Annu Rev Plant Biol 2003;54:109–36.
[59] Liu J, Wang W, Wu H, Gong X, Moriguchi T. Polyamines function in stress tolerance: from synthesis to regulation. Front Plant Sci 2015;6:827.
[60] Duan J, Li J, Guo S, Kang Y. Exogenous spermidine affects polyamine metabolism in salinity-stressed Cucumis sativus roots and enhances short-term salinity tolerance. J Plant Physiol 2008;165(15):1620–35.
[61] Wang B-Q, Zhang Q-F, Liu J-H, Li G-H. Overexpression of PtADC confers enhanced dehydration and drought tolerance in transgenic tobacco and tomato: effect on ROS elimination. Biochem Biophys Res Commun 2011;413 (1):10–6.
[62] Wen X-P, Ban Y, Inoue H, Matsuda N, Moriguchi T. Spermidine levels are implicated in heavy metal tolerance in a spermidine synthase overexpressing transgenic European pear by exerting antioxidant activities. Transgenic Res 2010;19(1):91–103.
[63] Huang X-S, Luo T, Fu X-Z, Fan Q-J, Liu J-H. Cloning and molecular characterization of a mitogen-activated protein kinase gene from Poncirus trifoliata whose ectopic expression confers dehydration/drought tolerance in transgenic tobacco. J Exp Bot 2011;62(14):5191–206.
[64] Gong X, Zhang J, Hu J, Wang W, Wu H, Zhang Q, et al. FcWRKY 70, a WRKY protein of *Fortunella crassifolia*, functions in drought tolerance and modulates putrescine synthesis by regulating arginine decarboxylase gene. Plant Cell Environ 2015;38(11):2248–62.
[65] Sun P, Zhu X, Huang X, Liu J-H. Overexpression of a stress-responsive MYB transcription factor of Poncirus trifoliata confers enhanced dehydration tolerance and increases polyamine biosynthesis. Plant Physiol Biochem 2014;78:71–9.
[66] Chen T, Li W, Hu X, Guo J, Liu A, Zhang B. A cotton MYB transcription factor, GbMYB5, is positively involved in plant adaptive response to drought stress. Plant Cell Physiol 2015;56(5):917–29.
[67] Wang F, Chen Z, Shabala S. Hypoxia Sensing in Plants: On a quest for ion channels as putative oxygen sensors. Plant Cell Physiol 2017;58:1126–42.
[68] Shabala S, Chen G, Chen Z-H, Pottosin I. The energy cost of the tonoplast futile sodium leak. New Phytol 2020;225(3):1105–10.
[69] Deng F, Zeng F, Chen G, Feng X, Riaz A, Wu X, et al. Metalloid hazards: from plant molecular evolution to mitigation strategies. J Hazard Mater 2021;409:124495.
[70] Xu J, Zhang S. Mitogen-activated protein kinase cascades in signaling plant growth and development. Trends Plant Sci 2015;20(1):56–64.
[71] Mare C, Mazzucotelli E, Crosatti C, Francia E, Stanca AM, Cattivelli L. Hv-WRKY38: a new transcription factor involved in cold-and drought-response in barley. Plant Mol Biol 2004;55:399–416.
[72] Ryu H-S, Han M, Lee S-K, Cho J-I, Ryoo N, Heu S, et al. A comprehensive expression analysis of the WRKY gene superfamily in rice plants during defense response. Plant Cell Rep 2006;25(8):836–47.
[73] Shen H, Liu C, Zhang Yi, Meng X, Zhou X, Chu C, et al. OsWRKY30 is activated by MAP kinases to confer drought tolerance in rice. Plant Mol Biol 2012;80 (3):241–53.
[74] G. Li, X. Meng, R. Wang, G. Mao, L. Han, Y. Liu, et al., Dual-level regulation of ACC synthase activity by MPK3/MPK6 cascade and its downstream WRKY transcription factor during ethylene induction in Arabidopsis, PLoS Genet. 8 (2012) e1002767.
[75] Wang P, Du Y, Zhao X, Miao Y, Song C-P. The MPK6-ERF6-ROS-responsive cis-acting Element7/GCC box complex modulates oxidative gene transcription and the oxidative response in Arabidopsis. Plant Physiol 2013;161(3):1392–408.
[76] Ueno D, Yamaji N, Kono I, Huang CF, Ando T, Yano M, et al. Gene limiting cadmium accumulation in rice. Proc Natl Acad Sci 2010;107(38):16500–5.
[77] Miyadate H, Adachi S, Hiraizumi A, Tezuka K, Nakazawa N, Kawamoto T, et al. OsHMA3, a P1B-type of ATPase affects root-to-shoot cadmium translocation in rice by mediating efflux into vacuoles. New Phytol 2011;189(1):190–9.
[78] Sharma SS, Dietz K-J, Mimura T. Vacuolar compartmentalization as indispensable component of heavy metal detoxification in plants. Plant Cell Environ 2016;39(5):1112–26.
[79] Sasaki A, Yamaji N, Ma JF. Overexpression of OsHMA3 enhances Cd tolerance and expression of Zn transporter genes in rice. J Exp Bot 2014;65(20):6013–21.
[80] Liu H, Zhao H, Wu L, Liu A, Zhao F-J, Xu W. Heavy metal ATPase 3 (HMA3) confers cadmium hypertolerance on the cadmium/zinc hyperaccumulator Sedum plumbizincicola. New Phytol 2017;215(2):687–98.